RESONANCE-ENHANCED MULTIPHOTON IONIZATION OF MOLECULAR HYDROGEN VIA THE E,F $^1\Sigma_g^+$ STATE: PHOTOELECTRON ENERGY AND ANGULAR DISTRIBUTIONS

Scott L. ANDERSON*, Glenn D. KUBIAK and Richard N. ZARE

Department of Chemistry, Stanford University, Stanford, California 94305, USA

Received 20 December 1983

Photoelectron energy and angular distributions are measured for the 2+1 multiphoton ionization process, H_2 X $^1\Sigma_g^+(v = 0, J) + 2h\nu \rightarrow$ E,F $^1\Sigma_g^+(v_E, J_E = J) + h\nu \rightarrow H_2^+$ X $^2\Sigma_g^+(v^+) + e^-$, for $v_E = 0, 1,$ or 2 and for $J_E = 0$ or 1 of the inner well of the double-minimum E,F state. Although a strong preference is found for $v^+ = v_E$, the detailed H_2^+ vibrational distribution does not exhibit Franck–Condon behavior, and the photoelectron angular distributions vary markedly with both the J_E value of the intermediate state and the v^+ value of the ion.

1. Introduction

Molecular hydrogen provides an important test system upon which a detailed understanding of molecular photoionization dynamics can be built. For this reason, there have been a number of experimental studies of the vacuum-ultraviolet photoionization of H_2 [1–9], a task requiring relatively narrow-band, high spectral brightness sources below 80 nm. Because H_2 is the simplest neutral molecule, the interpretation of photoionization experiments is the most advanced [10–12]. Of particular interest [8,13] is the role that autoionization plays in the angular and energy distributions of the ejected photoelectrons, since these ionizing resonances involve the coupling between nuclear and electronic motions ignored in a simple Born–Oppenheimer treatment.

It is also possible to use resonant multiphoton ionization (MPI) to study ionization of H_2 from various electronically excited states [14,15]. The selection rules governing multiphoton excitation make possible the study of states of symmetry identical or opposite to that of the ground state, depending on whether the number of photons absorbed is even or odd respectively. One such resonant MPI process

which has received recent attention involves the two-photon excitation E,F $^1\Sigma_g^+ \leftarrow$ X $^1\Sigma_g^+$ followed by subsequent absorption of one photon to cause ionization [14]. Fig. 1 shows a schematic diagram of the relevant potential curves and associated wavefunctions of the E,F state. This process has been studied both experimentally [14] and theoretically [17,18] and is of interest for at least two rather different reasons. The first reason is that the double-minimum nature of the intermediate E,F state should manifest itself in several ways in the ionization. For example, both the homogeneous perturbations between vibronic levels associated with the ionic inner (E state) and covalent outer (F state) wells and the expected large variation of the transition moment with H–H internuclear distance should cause interesting effects in the photoionization. The second reason is that this resonant 2+1 process is conveniently employed to determine internal-state populations of H_2 (and its isotopic variants) in molecular dynamics experiments involving gas-phase [19] and gas–surface scattering [20]. The most accurate and general use of this technique, however, requires that the details of the ionization process be known.

In the present study we report the energy and angular distributions of photoelectrons produced in the resonant 2+1 MPI of H_2 via the E,F state. We employ a time-of-flight (TOF) technique [21] to determine
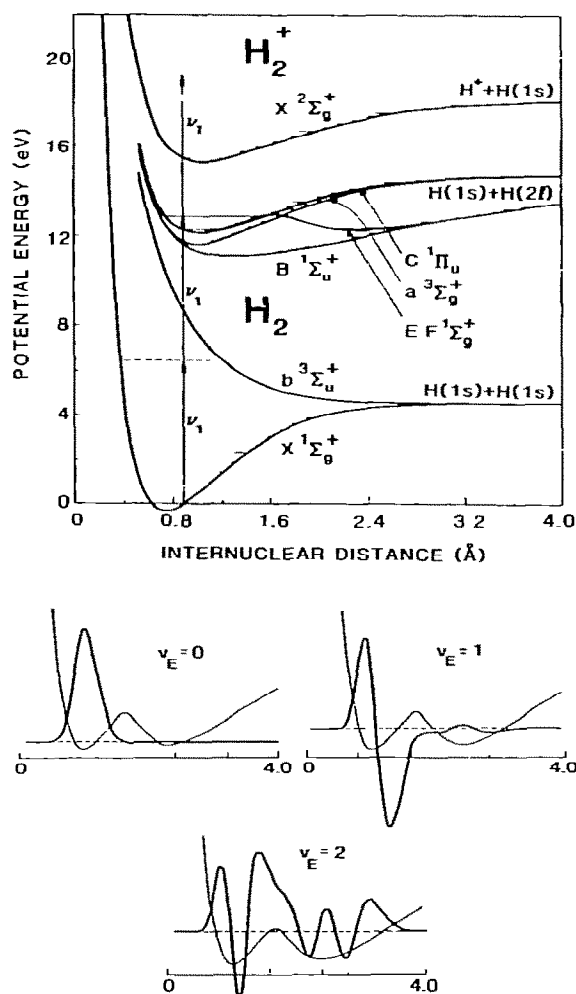

Fig. 1. Schematic potential-energy diagram for the ground and first three excited states of H_2 and the ground state of H_2^+. Also shown are wavefunctions calculated by Peek [16] for the three vibronic levels of the E (inner) potential well.

the photoelectron energies and use a rotating Fresnel rhomb to measure the angular distributions of the electrons as a function of (1) the final ionic vibrational level v^+ and (2) the rotational quantum number of the intermediate state, J_E. We perform measurements for excitation through each of the three bound vibronic levels of the inner or E well. We have adopted the convention of labeling these three levels as $v_E = 0$, 1 and 2 although they are in fact the levels $v = 0, 3$ and 6 of the full potential.

2. Experimental

High-intensity radiation tunable in the region from 193 to 202 nm is required to cause two-photon excitation to levels of the E,F state. These wavelengths are generated by frequency-doubling the output of a dye laser pumped by the second harmonic of a Nd^{3+}: YAG laser. The frequency-doubled dye laser is focused with a 60 cm focal-length quartz lens into a cell containing 5 atm of H_2 gas, thereby generating UV and VUV wavelengths via stimulated Raman scattering. The desired fourth anti-Stokes wave is separated from all other Stokes and anti-Stokes orders with a Pellin—Broca prism and then focused into the photoelectron spectrometer with a quartz lens having a focal length of 25 cm. Typical VUV pulse energies are 70–80 μJ into a bandwidth of 1.9 cm^{-1} representing a conversion efficiency of 1.2 $\times$ 10^{-3} based on the dye pulse energy. Beam quality is too poor to estimate meaningfully the effective power densities. Laser polarization is normally parallel to the detection axis of the photoelectron spectrometer. Photoelectron angular distributions are measured by rotating the laser polarization with respect to the (fixed) detector axis using a double Fresnel rhomb retarder which attenuates the fourth anti-Stokes beam energy by $\approx 40\%$.

Photoelectron energies are measured in a time-of-flight spectrometer which has been briefly described [22]; only improvements incorporated in the spectrometer will be summarized here. The stainless-steel vacuum system now contains a double-wall mu-metal flight tube, the inside of which is graphite-coated. The system is evacuated through a mu-metal baffle by a 110 ℓ/s turbo pump and its flight tube is divided by a conical baffle which serves to reduce the background signal level arising from scattered light and photoelectrons. Hydrogen gas is sampled from a pulsed free jet expansion. The pulsed valve (Lasertechnics LPV) is located just outside the mu-metal flight tube, ≈ 5 cm from the axis. Typical operating conditions are: stagnation pressure of ≈ 200 Torr, 0.3 mm nozzle diameter, ≈ 150 μs temporal pulse width fwhm, time-averaged background pressure of 2 $\times$ 10^{-6} Torr and an estimated laser—jet interaction region pressure of $\approx 10^{-3}$ Torr. Ionization occurs on the axis of the flight tube at the intersection of the free jet and the laser focal volume. The electron detector, a channel electron multiplier array with 50 ohm anode (Galileo

FTD 2003) is located at the other end of the flight tube, separated from the field-free region by a double shielding grid. The field-free flight path is 50 cm.

No collection or acceleration fields are used in these experiments; thus the detection efficiency ($\approx 5 \times 10^{-4}$) is determined by the solid angle subtended by the detector. Electron TOF distributions are collected after amplification of the detector output and are stored in a Tektronix 7912AD transient digitizer. Arrival times range from a few hundred nanoseconds to nearly 5 μs, depending on electron energy. Resolution in these experiments is ≈ 150 meV due to the combined effects of timing resolution and space-charge broadening.

The spectral transformation from time to energy is accomplished with the aid of a computer. The energy scale is determined by calibration to MPI photoelectron spectra of xenon and iron, the source of the latter being the photodissociation of iron pentacarbonyl [22]. The spectra reported here are not corrected for any dependence of transmission on photoelectron energy. This is believed to be a small effect since all measured spectral features are well above the transmission cut-off for the instrument (0.1 eV).

3. Results and discussion

We have measured the TOF spectra of photoelectrons produced in the photoionization of H_2 through the three vibronic levels of the inner well of the E,F $^1\Sigma_g^+$ state. Fig. 2 presents the resulting photoelectron energy spectra. It should be noted that the signal immediately to lower energy (longer arrival time) of the largest peak in each spectrum is somewhat distorted by ringing of the detection system following the sharp (9 ns fwhm) main peak. An attempt to correct for this by subtraction of the similar ringing waveform observed in MPI photoelectron spectra of Xe was unsuccessful but suggests that the effect on peak heights in the H_2 spectra is less than 10%.

The most obvious feature in each of the three spectra of fig. 2 is that the most probable final ion vibrational level, v^+, is indentical to the intermediate vibronic level of the E,F state. Fig. 1 shows that in all cases there is sufficient energy in the ionization process to populate all the bound vibrational levels of H_2^+ and even to cause dissociation. However, the strong
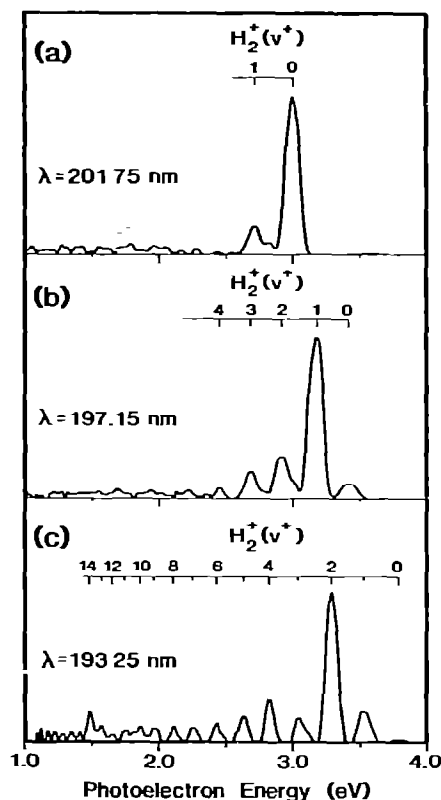

Fig. 2. Photoelectron spectra following ionization via the three vibronic levels of the two-photon resonant intermediate E,F $^1\Sigma_g^+$ state of H_2: (a) H_2 $^1\Sigma_g^+(v = 0, J = 0) + 2h\nu \rightarrow H_2$ E,F$(v_E = 0, J_E = 0) + h\nu \rightarrow H_2^+ X\,^2\Sigma_g(v^+, J^+)$; (b) H_2 $^1\Sigma_g^+(v = 0, J = 1) + 2h\nu \rightarrow H_2$ E,F$(v_E = 1, J_E = 1) + h\nu \rightarrow H_2^+ X\,^2\Sigma_g(v^+, J^+)$; and (c) H_2 $^1\Sigma_g^+(v = 0, J = 1) + 2h\nu \rightarrow H_2$ E,F$(v_E = 1, J_E = 1) + h\nu \rightarrow H_2^+ X\,^2\Sigma_g(v^+, J^+)$.

preference for the diagonal $v^+ = v_E$ transition is expected qualitatively from application of the Franck–Condon principle to the H_2 E, F and H_2^+ X potential curves.

It is also observed that there is a non-negligible fraction of structureless photoelectron intensity at low energy. The intensity of this broad background is sensitively dependent on both the alignment of the laser with respect to the light baffles and also on the background pressure of H_2, suggesting that this fraction of the photoelectron flux is produced by the chamber walls or perhaps by collisions of H_2 photoelectrons with background gas molecules near the jet.

It is doubtful that this background can be attributed to dissociative ionization, i.e. the process $H_2 + h\nu \rightarrow H^+ + H + e^-$. Using a separate apparatus which incorporates a TOF mass spectrometer, we are able to support this contention by noting that the upper limit to dissociative ionization based on the appearance of the H^+ mass is 5% when a similar ionization process is employed, although with tighter focusing conditions and all anti-Stokes wavelengths.

Quantitative attempts to understand the observed υ^+ distributions were made by employing overlap integrals between wavefunctions associated with the three E well vibrational levels and those associated with the X state of the ion as calculated by Peek [16]. The wavefunctions corresponding to the H_2 E,F and H_2^+ X state potentials were generated from the potentials of Kołos and Wolniewicz [23] and Beckel et al. [24] respectively. The values of these overlap integrals were then squared and weighted by the quantity ϵ^{-1} where ϵ is the final photoelectron energy corresponding to a given υ^+. Previous calculations by O'Neil and Reinhardt [12] on photoionization of the H_2 X state demonstrate that the above prescription is accurate to within 8% of a more complete calculation

Table 1
Comparison of experimental [a] and calculated ion vibrational distributions. Entries less than 10^{-3} are not listed

υ^+	υ_E					
	0_{expt}	0_{calc}	1_{expt}	1_{calc}	2_{expt}	2_{calc}
0	0.865	0.963	0.073	0.031	0.007	–
1	0.135	0.035	0.580	0.910	0.072	0.032
2	–	0.002	0.208	0.048	0.396	0.633
3	–	–	0.102	0.011	0.074	0.001
4	–	–	0.038	–	0.100	0.045
5	–	–	–	0.001	0.058	0.001
6	–	–	–	–	0.044	0.002
7	–	–	–	–	0.030	0.016
8	–	–	–	–	0.034	–
9	–	–	–	–	0.029	0.016
10	–	–	–	–	0.035	–
11	–	–	–	–	0.024	0.017
12	–	–	–	–	0.016	0.036
13	–	–	–	–	0.028	0.175
14–16	–	–	–	–	0.054	0.026

[a] Note that except for $\upsilon_E = 1$ the tabulated quantities are *not* corrected for the dependence of the angular distribution on ion vibrational level.

which includes a radial as well as photoelectron-energy-dependent transition moment. The ϵ^{-1} weighting may account for the sharp increase in the electronic transition moment with decreasing photoelectron energy, although the true E $\rightarrow$ X weighting may differ from this form.

Table 1 lists the normalized experimental υ^+ distributions and those calculated in this manner It is clear from table 1 that the simple Franck—Condon calculation overestimates the variation with υ^+ and does not reproduce the distribution of ion vibrational levels measured. The electronic transition moment between the broad E,F state and the X state of the ion is expected to have a large dependence on internuclear separation which, to our knowledge, has not been calculated The υ^+ dependent photoelectron angular distributions, which are discussed below, also indicate the existence of interactions between the departing electron and the vibrating ion core, ignored in the Franck—Condon picture.

In fig. 3, we show angular distributions measured for each of the five υ^+ levels detectable in the photoelectron spectra of H_2 ionized via the Q_0 and Q_1 excitation lines of the (1, 0) band. The results were obtained by rotating the retarder through 2π, averaging the data into one quadrant and reflecting that one quadrant across $\theta = 0$ to form fig. 3. Quick inspection of this figure shows that there are significant variations in the distributions as a function of υ^+ and as a function of the intermediate rotational quantum number. In the general case of a three-photon ionization process the angular distribution can include even Legendre polynomials up to $P_6(\cos\theta)$. However, because we are investigating a resonant 2 + 1 multiphoton ionization, this description may be simplified. In particular for Q_0 excitation, the $J_E = 0, M_E = 0$ intermediate level is isotropic and the photoelectron distribution can only be of the form $1 + \beta P_2(\cos\theta)$. On the other hand for Q_1 excitation, the $J_E = 1, M_E = 0, \pm 1$ intermediate levels may be aligned and the photoelectron distribution can have the form [25] $1 + \beta P_2(\cos\theta) + \gamma P_4(\cos\theta)$. This is borne out by the fact that attempting to fit the Q_0 data with both β and γ yields γ values no larger than 3% of the β values. In contrast, ionization of the aligned E,F $J_E = 1$ level exhibits angular properties which contain higher moments of $\cos\theta$ and typical γ values are $\approx 30\%$ of the β values for a given distribution.
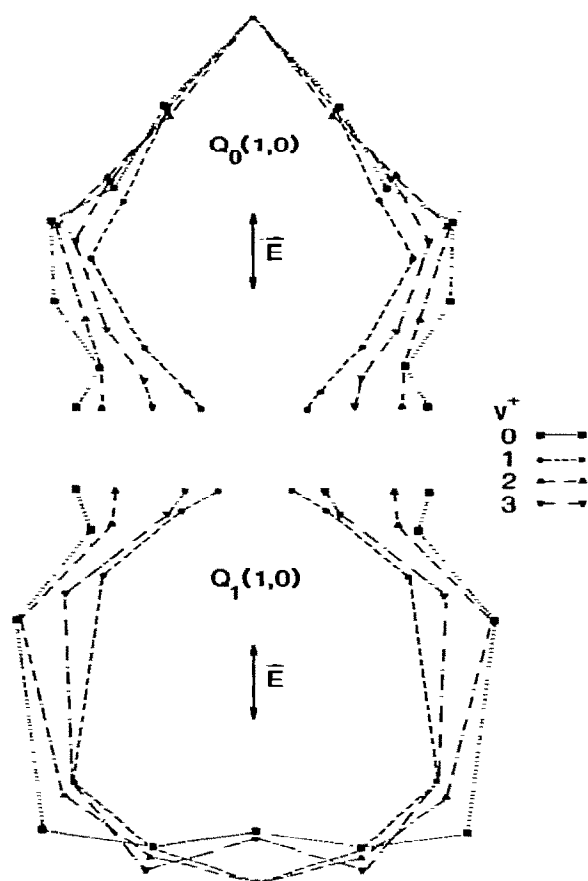
Fig. 3. Angular distributions of photoelectrons associated with the final H_2^+ ion levels $v^+ = 0-3$ for ionization via the process $E,F \, ^1\Sigma_g^+(v_E = 1) \leftarrow X \, ^1\Sigma_g^+(v = 0)$. Data are presented for ionization via both the Q_0 and Q_1 excitation lines.

Table 2 gives the values of β and γ for $v^+ = 0-3$ when both Q_0 and Q_1 excitation are employed. It is expected on theoretical grounds that the angular distribution can vary with laser intensity [26], but no systematic studies of this kind were attempted. Fig. 4 compares the measured and best-fit angular distributions for $v^+ = 1$ for ionization via Q_0 or Q_1 excitation. For Q_0 excitation the measured distribution is clearly much sharper than the best-fit even though terms higher than $\cos^2\theta$ are not expected. This probably represents the presence of systematic errors in the data, perhaps caused by changes in the laser beam shape and direction as the retarder is rotated. Nonetheless, it is clear that there exist significant differences between the various v^+ angular distributions.
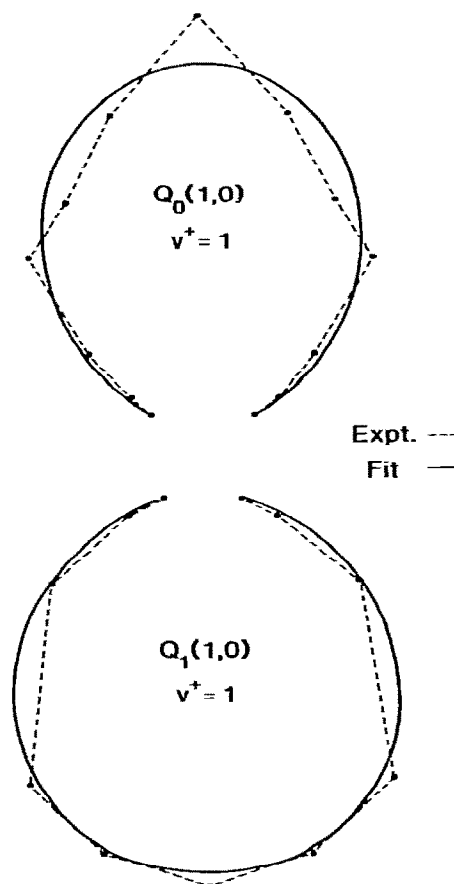

Fig. 4. Comparison of experimental and best-fit angular distributions for $v^+ = 1$ produced in the Q_0 and Q_1 excitation processes of fig. 3. The corresponding β and γ parameters can be found in table 2.

Table 2

Best-fit photoelectron angular distribution parameters [a]

E,F v^+	$v' = 1$ β	$J = 0$ γ	E,F v^+	$v' = 1$ β	$J = 1$ γ
0	0.59	0	0	0.71	−0.32
1	1.29	0	1	1.34	−0.18
2	0.75	0	2	0.85	−0.23
3	0.68	0	3	1.02	−0.28

[a] An accuracy of 30% or 0.1, whichever is greater, has been assigned to the β and γ parameters.

A full investigation of the vibrational-dependent angular distributions suggests the use of a two-color experiment in which the two-photon resonance wavelength of the final ionization step is varied. Indeed, we have carried out preliminary experiments of this kind, using various combinations of the fixed anti-Stokes wavelengths as the two colors. Ample signal-to-noise is readily achieved, owing in part to the relatively long lifetime (100 ± 20 ns) of the H_2 E,F state [27]. The feasibility of this experiment suggests that the photoionization dynamics of H_2 can be investigated in the detail appropriate to this simplest of all molecules.

References

[1] H. Beutler, Z. Physik. Chem. (Frankfurt) B29 (1935) 315;
H. Beutler, A. Deubner and H.O. Junger, Z. Physik 98 (1936) 181;
H. Beutler and H.O. Junger, Z. Physik 100 (1936) 80; 101 (1936) 285, 304.

[2] G.R. Cook and P.H. Metzger, J. Op. Soc. Am. 54 (1964) 968.

[3] V.H. Dibeler, R.M. Reese and M. Krauss, J. Chem. Phys. 42 (1965) 2045.

[4] F.J. Comes and H.O. Wellern, Z. Naturforsch. 23a (1968) 881

[5] W.A. Chupka and J. Berkowitz, J. Chem. Phys. 51 (1969) 4244.

[6] S. Takezawa, J. Chem. Phys. 52 (1970) 2575, 5793.

[7] G. Herzberg and Ch. Jungen, J. Mol. Spectry. 41 (1972) 425.

[8] P.M Dehmer and W A. Chupka, J. Chem. Phys. 65 (1976) 2243; 66 (1977) 1972; 79 (1983) 1569.

[9] J.E.P ollard, D.J. Trevor, J.E. Reutl. Y.T. Lee and D.A. Shirley, Chem. Phys. Letters 88 (1982) 434; J. Chem. Phys. 77 (1982) 34;
J.E. Pollard, D J Trevor, Y.T. Lee and D A. Shirley, J. Chem. Phys. 77 (1982) 4818.

[10] U. Fano, Phys Rev. A2 (1970) 353.

[11] Ch. Jungen and O. Atabek, J Chem. Phys. 66 (1977) 5583.

[12] S.V. O'Neil and W.P. Reinhardt, J. Chem Phys. 69 (1978) 2126.

[13] O. Atabek, D. Dill and Ch. Jungen, Phys. Rev. Letters 33 (1974) 123;
O. Atabek and Ch. Jungen, in: Electron and photon interactions with atoms, eds H. Kleinpoppen and M.R.C. McDowell (Plenum Press, New York, 1976);
M Raoult, Ch. Jungen and D. Dill, J. Chim Phys. Phys. Chim Biol. 77 (1980) 599;
D. Dill and Ch. Jungen, J. Phys. Chem. 84 (1980) 2116,
M. Raoult and Ch. Jungen, J. Chem. Phys. 74 (1981) 3883;
Ch. Jungen and M. Raoult, Faraday Discussions Chem Soc. 71 (1981) 253;
K. Rai Dastidar and P. Lambropoulos, Chem. Phys. Letters 93 (1982) 273;
K. Rai Dastidar, Chem. Phys. Letters 101 (1983) 255.

[14] E.E. Marinero, C.T. Rettner and R.N. Zare, Phys. Rev. Letters 48 (1982) 1323;
E.E. Marinero, R. Vasudev and R.N. Zare, J. Chem. Phys. 78 (1983) 692.

[15] S.T Pratt, P.M. Dehmer and J.L. Dehmer, J. Chem. Phys. 78 (1983) 4315, to be published.

[16] J.M. Peek, unpublished

[17] B Ritchie, E.J. McGuire, J.M. Peek and C.W. Hand, J. Chem. Phys. 77 (1982) 877.

[18] W.M. Huo and R.L. Jaffe, Chem. Phys Letters 101 (1983) 463

[19] C.T. Rettner, E.E. Marinero and R.N. Zare, in: Physics of Electronic and Atomic Collisions, Invited papers from the XIIIth ICPEAC, Berlin, 1983, eds. J. Eichler, I.V. Hertel and N. Stolterfoht (North-Holland, Amsterdam), to be published.

[20] G.D. Kubiak, G.O Sitz, J.E. Hurst Jr. and R.N. Zare, Book of Abstracts, ACS National Meeting, Washington, D.C., August, 1983.

[21] M.G. White, R.A. Rosenberg, G. Gabor, E.D. Poliakoff, G. Thornton, S.H. Southworth and D.A. Shirley, Rev. Sci. Instr. 50 (1979) 1268.

[22] S.L. Anderson, D.M. Rider and R.N. Zare, Chem. Phys. Letters 93 (1982) 11.

[23] W. Kolos and L. Wolniewicz, J. Chem. Phys. 50 (1969) 3228.

[24] C.L. Beckel, B.D. Hansen and J.M. Peek, J. Chem. Phys. 53 (1970) 3681.

[25] P. Lambropoulos, Advan. At. Mol Phys. 12 (1976) 87.

[26] S.N. Dixit and P. Lambropoulos, Phys. Rev. A27 (1983) 861.

[27] D.J. Kligler and C.K. Rodes, Phys. Rev. Letters 40 (1983) 861.

[27] D.J. Kligler and C.K. Rhodes, Phys. Rev. Letters 40 (1978) 309;
D.J. Kligler, J. Bokor and C.K. Rhodes, Phys. Rev. A21 (1980) 607.